Electronic Supplementary Material (ESI) for Physical Chemistry Chemical Physics.
This journal is © the Owner Societies 2024

SUPPLEMENTAL INFORMATION

Incorporating Solvent Effects in DFT: Insights from Cation Exchange in Faujasites

An T. Ta[1], Ayoub Daouli[2], R. Seaton Ullberg[1], Eric Fonseca[1], Vanessa Proust[3], Agnès Grandjean[3], Richard G. Hennig[1], Michael Badawi[2, †] Simon R. Phillpot[1, †]

[1]Department of Materials Science and Engineering, University of Florida, Gainesville, FL 32611
[2] Laboratory of Molecular Chemistry, University of Lorraine, 54000 Nancy, France
[3] CEA, DES, ISEC, DMRC, Univ Montpellier, Marcoule, France
[†]Corresponding authors: michael.badawi@univ-lorraine.fr; sphil@mse.ufl.edu

Contents

Explicitly solvated zeolite models

Table S1 reports the composition of zeolite structures containing three active-site waters (AHN = 3) and non-active site hydration numbers (NAHN) of 1 or 2. Note that a unique model is required for site II and site III exchange process, respectively. For each case, cif files have also been provided for reference. The procedural steps taken to generate explicitly solvated zeolite models as described in Section 2.3 and 3.1 (AHN = 3) of the manuscript are outlined below.

1. Optimize hydrated Na-X zeolite structure.
    a. Full ionic relaxation is performed on structures containing the desired AHN and NAHN.
    b. Two Na-X structures were generated: one where the active site is at site II and the other where the active site is at site III.
2. Selective dynamic optimization of ion exchanged Na-X zeolite.
    a. Replace active site Na^+ in optimized structure from step (1) with $Li^+/K^+/Rb^+$.
    b. Constrain non-active site waters using selective dynamics such that only ions and water molecules at the active sites are allowed to move during ionic relaxation.
        - Relaxed structures consistently have AHN = 3 for all exchanged zeolites.

Table S1. Chemical compositions for explicitly hydrated structure models used for site II and site III exchange processes, respectively, for cases where NAHN = 1 or 2.

NAHN	site exchange process	chemical composition
1	II	$MNa_{19}Al_{20}Si_{28}O_{96} \cdot 14\, H_2O$ (M = Na, K)
2	II	$MNa_{19}Al_{20}Si_{28}O_{96} \cdot 25\, H_2O$ (M = Na, Li, K, Rb)
1	III	$MNa_{19}Al_{20}Si_{28}O_{96} \cdot 12\, H_2O$ (M = Na, K)
2	III	$MNa_{19}Al_{20}Si_{28}O_{96} \cdot 24\, H_2O$ (M = Na, Li, K, Rb)

Chemical potentials

Table S2. Calculated standard chemical potential of cations in vacuum and water.

ion	$\mu^0_{A,(g)}$ (eV)	$\mu^0_{A,(aq)}$ (eV)
Na^+	5.131	-2.165
Li^+	5.290	-2.141
K^+	4.290	-2.361
Rb^+	4.130	-2.384

Li^+ exchange energies

In the case of Li^+ containing exchange processes, calculations within implicit water were preliminarily calculated using an explicit cut-off charge density parameter, η_c, set to 2.5×10^{-4} $Å^{-3}$. This parameter selection was informed by prior PCM studies on Li^+ battery systems[1,2]. It should be emphasized that results reported herein should be interpreted with caution as optimization studies are needed to establish confidence in the value of η_c and, possibly other parameter settings for appropriate treatment of Li atoms in the VASPsol PCM model. Explicitly solvated Li^+ ion reference states contained 4 coordinated water molecules which was derived from experimental characterization[3].

Figure S1 presents the predicted exchange energies for Li^+. When adopting the D and EI method, analysis reveals that only site II exhibits favorable exchange. In contrast, the E and I methods both predict unfavorable Li^+ exchange at sites II and III.

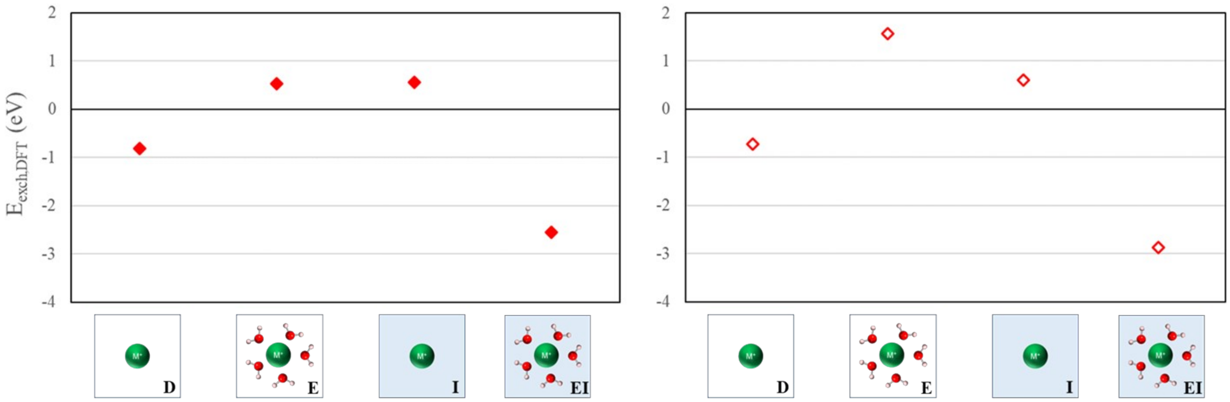

Figure S1. Site II (left) and site III (right) Li^+ exchange energies predicted from calculations using various reference states to model the exchange process. Labels and images describe the type of reference state used for zeolite and ions as described in Figure 3.

Figure S2 shows the energy differences between Li^+ exchange at site II versus III. In terms of qualitative predictions, the D and E method align together in predicting significant preference for Li^+ exchange at site II. Conversely, the I method predicts little favorability towards site II or III while the EI method indicates that exchange is preferred in site III.

Figures S3 show the Li^+ exchange energies for site II and site III using semi-empirical calculations, respectively. Contrary to predictions made for K^+/Rb^+ exchange, most modeling methods for zeolite reference states yielded favorable exchange for Li^+. The most favorable exchange was observed when using the EI method and unfavorable exchange was predicted for site III only when using the E method. Figure S4 illustrates the energetic differences between site II and III exchange which shows qualitative prediction to be nearly identical to pure DFT results (Figure S2). This is also supported by a parity plot depicting the similarity/differences between

DFT and semi-empirical predictions on relative site exchange which is also reported in Figure S4.

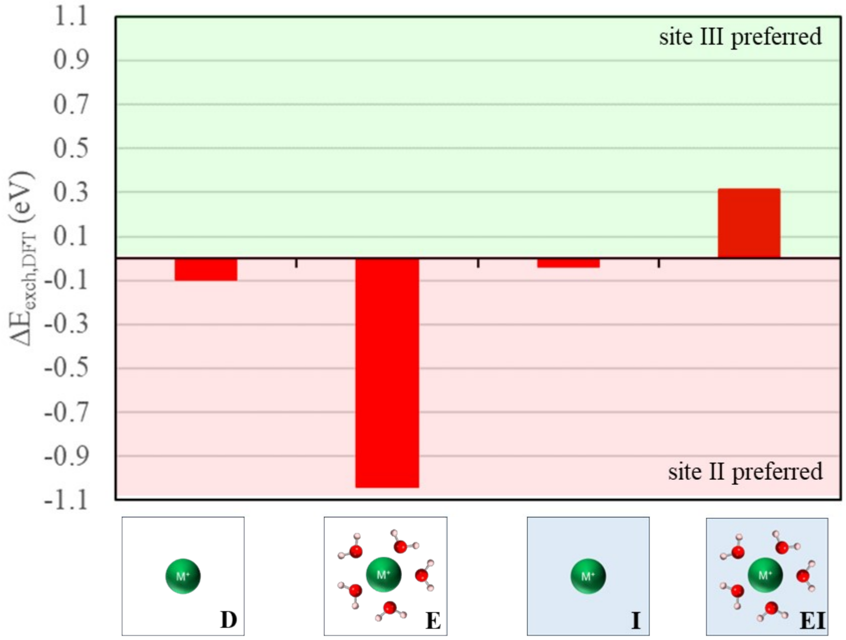

Figure S2. Energy differences between site II and site III Li$^+$ exchange in Na-X predicted from calculations using various reference states to model the exchange process. Labels and images describe the type of reference state used for zeolite and ions as described in Figure 3.

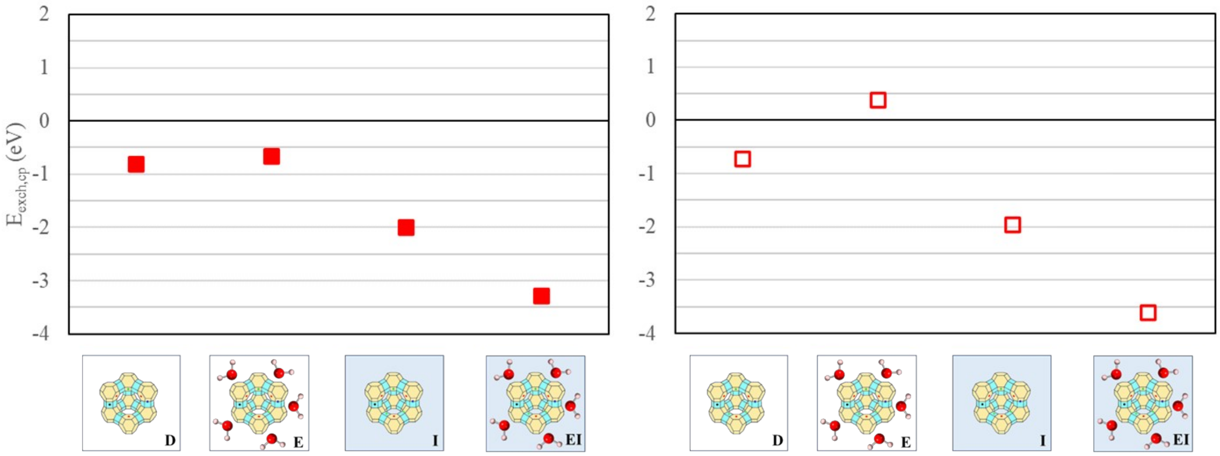

Figure S3. Site II (left) and site III (right) Li$^+$ exchange energies predicted from semi-empirical calculations using various zeolite reference states. Labels denote the specific reference state employed (Figure 3) and the images denote that only zeolite reference states were modeled with DFT.

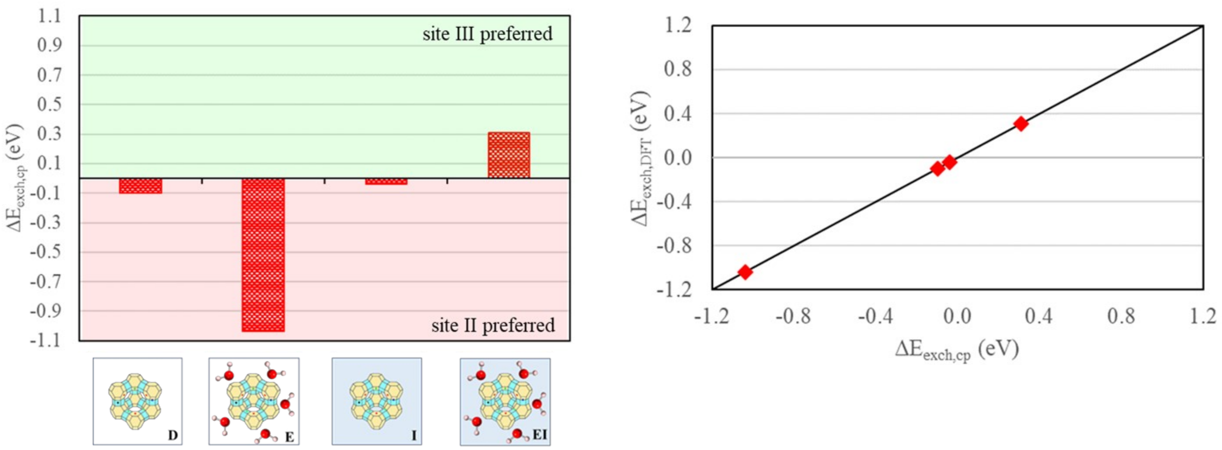

Figure S4. Differences between site II and site III Li^+ exchange energies predicted from semi-empirical calculations using various zeolite reference states (left) and parity plot of predicted exchange energy differences between sites using pure DFT and semi-empirical calculation (right). Labels denote the specific reference state employed (Figure 3) and the images denote that only zeolite reference states were modeled with DFT.

K^+ and Rb^+ exchange energy differences (semi-empirical)

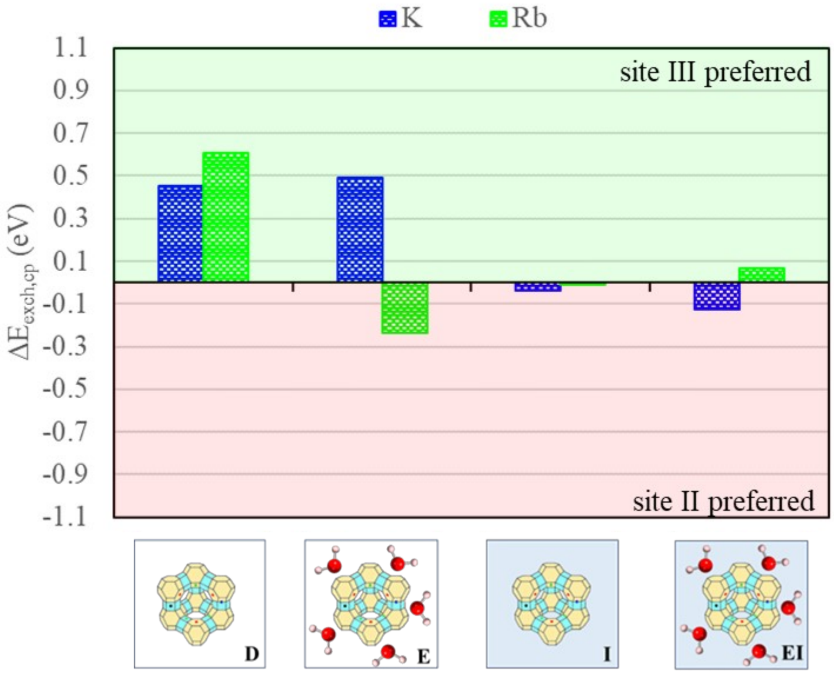

Figure S5. Differences between site II and site III K^+ and Rb^+ exchange energies predicted from semi-empirical calculations using various zeolite reference states. Labels denote the specific reference state employed (Figure 3) and the images denote that only zeolite reference states were modeled with DFT.

Comprehensive exchange energies (DFT)

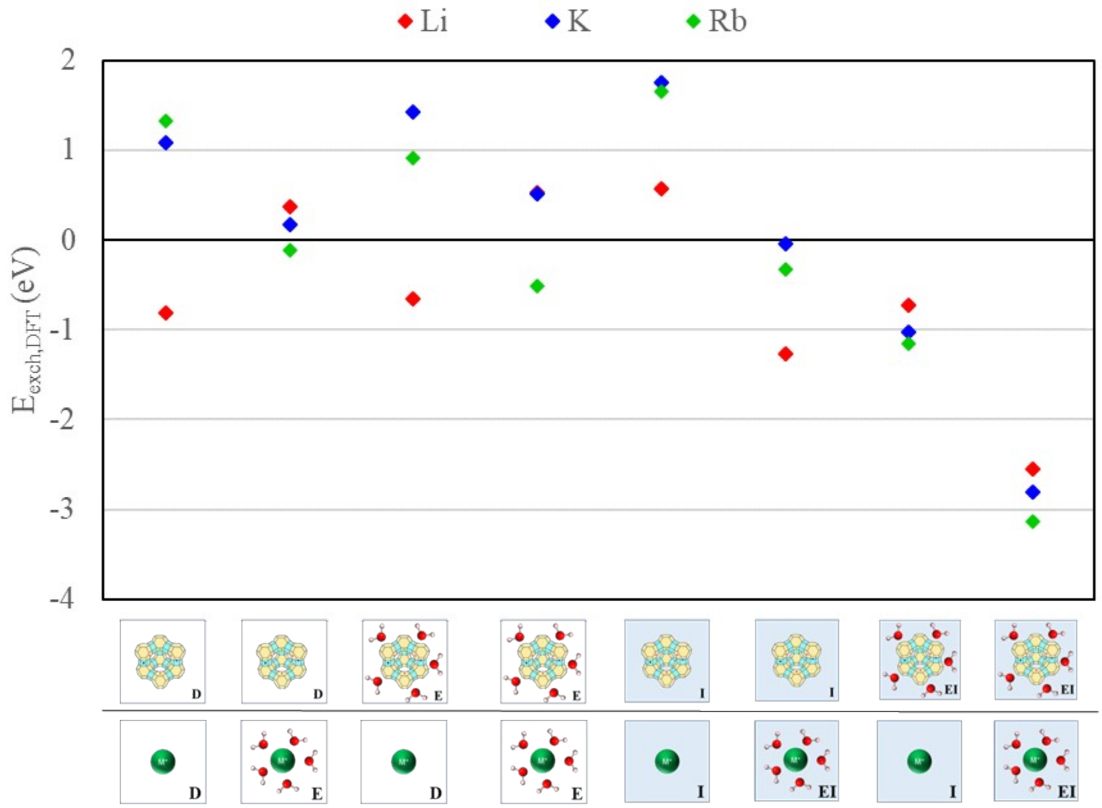

Figure S6. Site II exchange energies predicted from DFT calculations using various reference states to model the exchange process. Labels and images describe the type of reference state used for zeolite and ions as described in Figure 3.

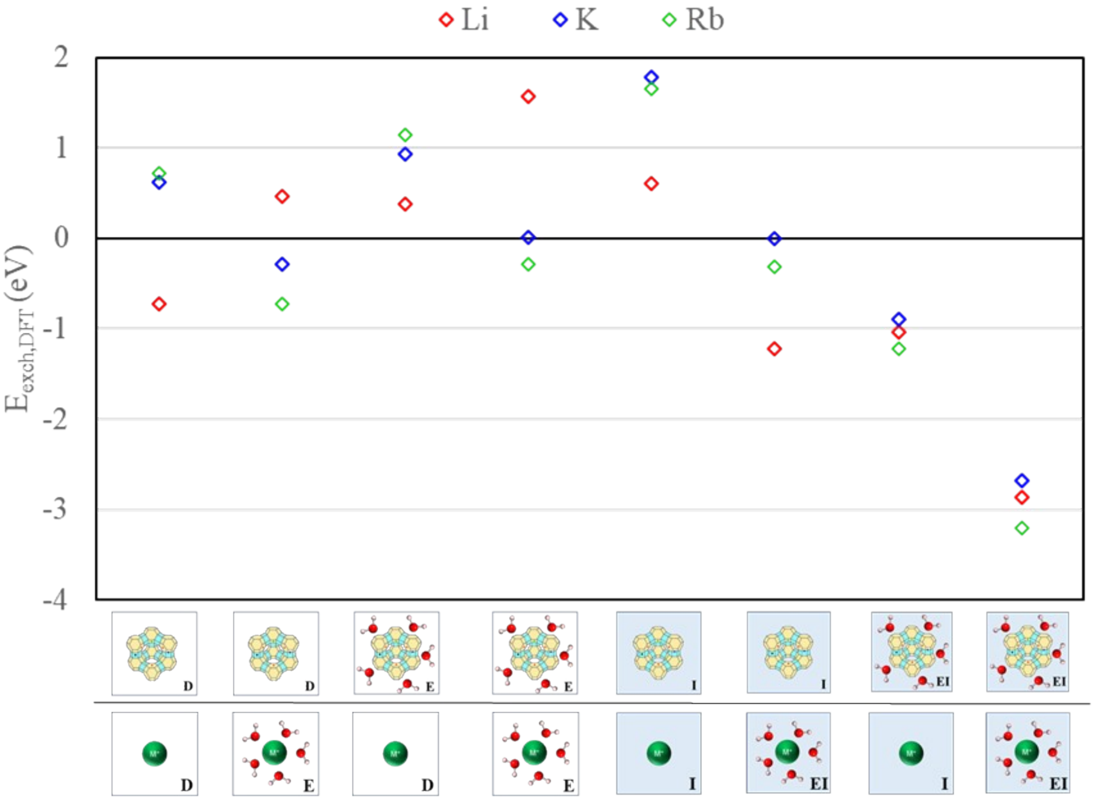

Figure S7. Site III exchange energies predicted from DFT calculations using various reference states to model the exchange process. Labels and images describe the type of reference state used for zeolite and ions as described in Figure 3.

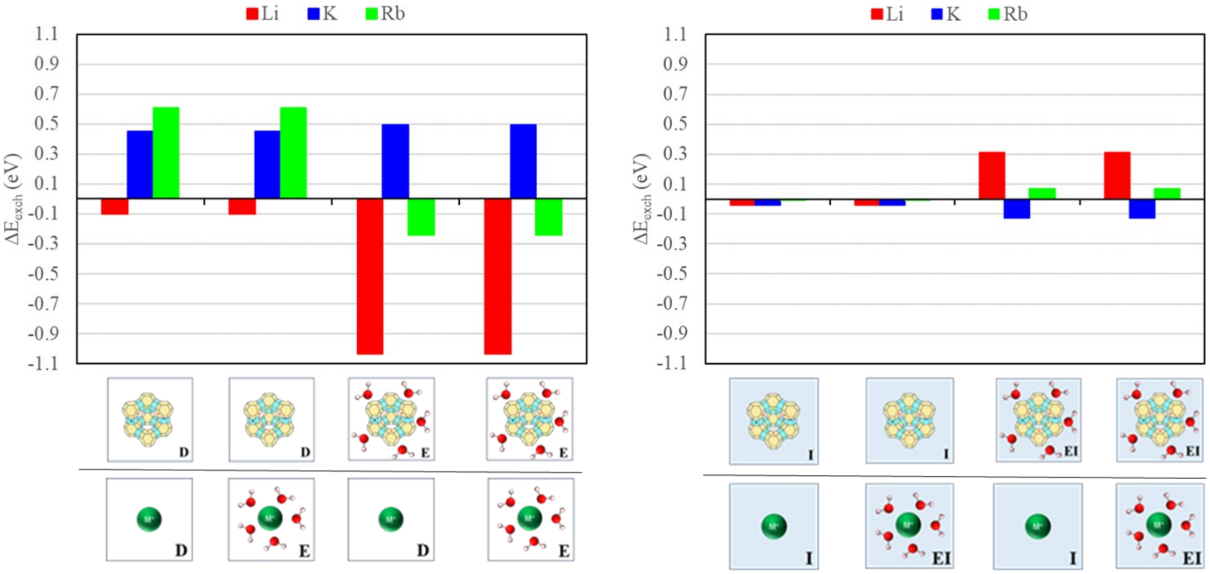

Figure S8. Energy differences between site II and site III cation exchange in Na-X predicted from DFT calculations using various reference states to model the exchange process. Labels and images describe the type of reference state used for zeolite and ions as described in Figure 3.

Reference state total energies (DFT)

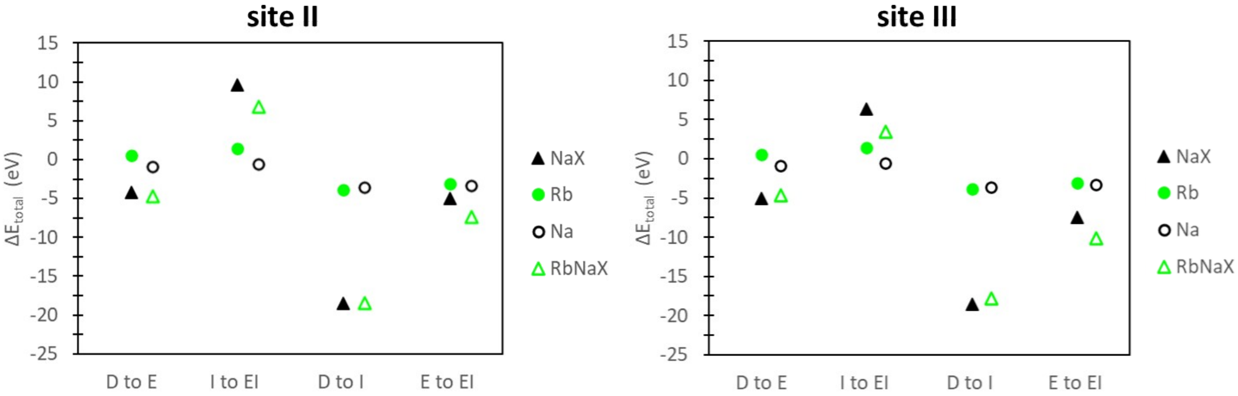

Figure S9. Change in total energy of reference states when comparing different modeling approaches used for calculating the exchange energy of Rb^+ with Na-X in site II (left) and site III (right). Closed symbols denote total energies of reactants while open symbols denote total energies of products in the exchange process.

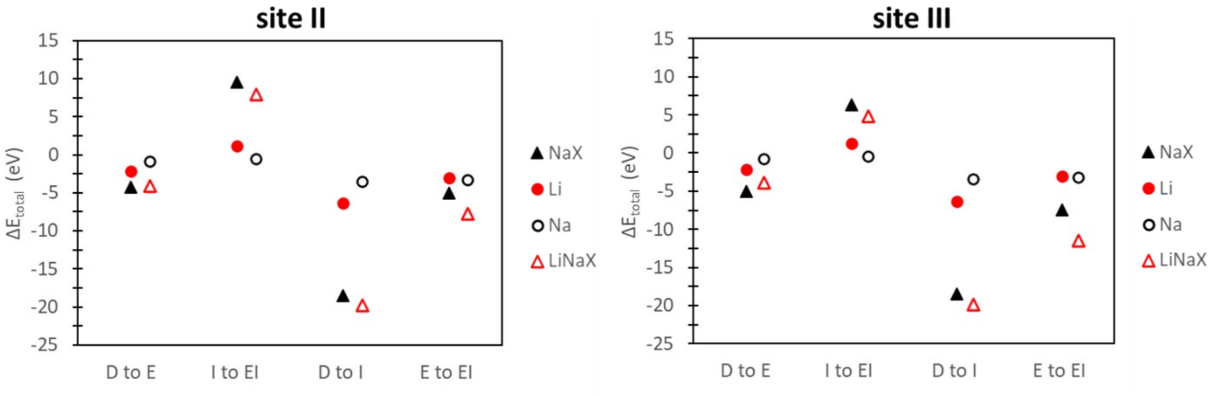

Figure S10. Change in total energies of reference states when comparing different modeling approaches used for calculating the exchange energy of Li$^+$ with Na-X in site II (left) and site III (right). Closed symbols denote total energies of reactants while open symbols denote total energies of products in the exchange process.

Table S3. Total energies (eV) of reference states used to calculate E_{exch}.

species	**D**	**E**	**I**	**EI**
ion and water reference states				
Na$^+$	5.131	-55.257[a]	1.534	-58.659[a]
Li$^+$	5.290	-56.360[a]	-1.005	-59.372[a]
K$^+$	4.290	-55.257[a]	0.079	-58.327[a]
Rb$^+$	4.130	-114.441[b]	0.259	-117.556[b]
site II zeolite reference states				
Na$_{20}$-X	-1191.813	-1568.190[c]	-1210.309	-1573.217[c]
Li$_1$Na$_{19}$-X	-1192.473	-1568.688[c]	-1212.285	-1576.487[c]
K$_1$Na$_{19}$-X	-1191.578	-1567.609[c]	-1210.019	-1575.693[c]
Rb$_1$Na$_{19}$-X	-1191.492	-1568.279[c]	-1209.930	-1575.646[c]
site III zeolite reference states				
Na$_{20}$-X	-1191.813	-1554.116[d]	-1210.309	-1561.552[d]
Li$_1$Na$_{19}$-X	-1192.374	-1553.577[d]	-1212.246	-1565.133[d]
K$_1$Na$_{19}$-X	-1192.028	-1554.029[d]	-1209.979	-1563.904[d]
Rb$_1$Na$_{19}$-X	-1192.100	-1553.966[d]	-1209.922	-1564.049[d]

[a] reference states include 4 water molecules whose total energies are -14.886 eV and -14.900 eV for calculations in vacuum and VASPsol, respectively.

[b] Rb$^+$ reference state includes 8 water molecules .

[c] Hydrated zeolite reference states used for site II exchange contains 25 water molecules.

[d] Hydrated zeolite reference states used for site III exchange contains 24 water molecules.

Metal-O_w bond distances in ion reference states

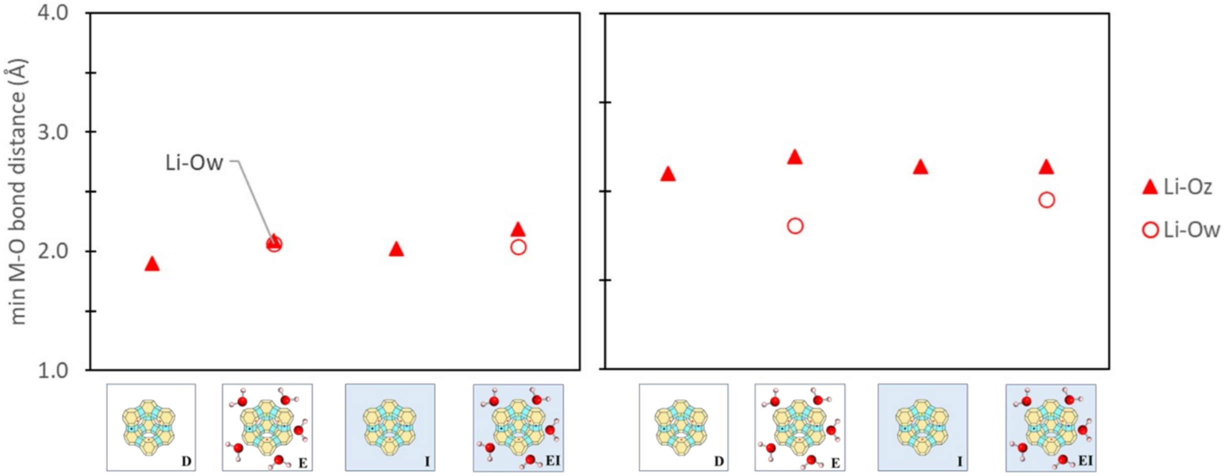

Figure S11. Minimum Li^+-to-oxygen bond distances between the Li^+-zeolite oxygen (Li-O_z) and Li^+-water oxygen (Li-O_w) in zeolite site II (left) and site III (right) reference states. Labels denote the specific reference state employed (Figure 3) and the images denote that only zeolite reference states are being analyzed.

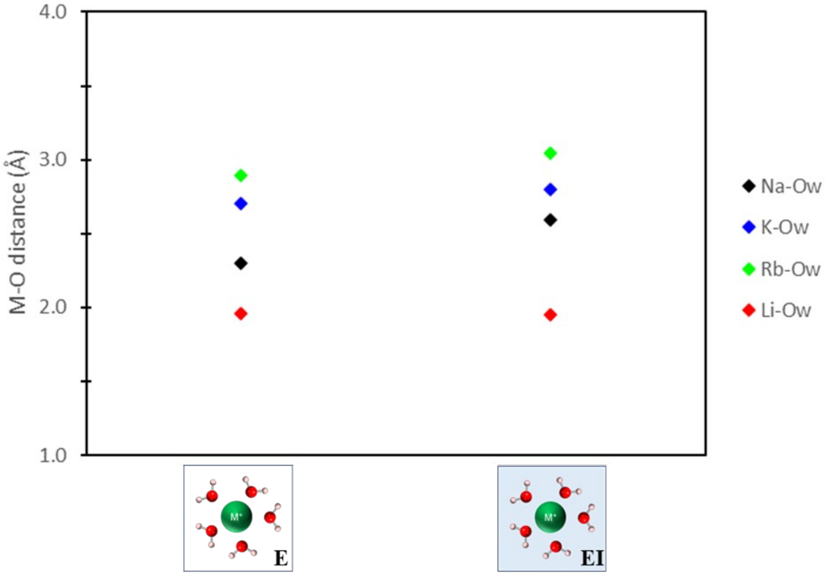

Figure S12. Minimum cation-to-oxygen bond distances between the cation and water oxygens in ion reference states. Labels denote the specific reference state employed (Figure 3).